Journal of African Earth Sciences 143 (2018) 187–194

Contents lists available at ScienceDirect

Journal of African Earth Sciences

journal homepage: www.elsevier.com/locate/jafrearsci

The 03 April 2017 Botswana M6.5 earthquake: Preliminary results

Vunganai Midzi [a,*], I. Saunders [a], B. Manzunzu [a], M.T. Kwadiba [b], V. Jele [a], R. Mantsha [a], K.T. Marimira [c], T.F. Mulabisana [a], O. Ntibinyane [b], T. Pule [a], G.W. Rathod [a], M. Sitali [d], L. Tabane [a], G. van Aswegen [a], B.S. Zulu [a]

[a] Council for Geoscience, Engineering and Geohazards Unit, Silverton, Pretoria, South Africa
[b] Botswana Geoscience Institute, Lobatse, Botswana
[c] Meteorological Services Department, Goetz Observatory, Bulawayo, Zimbabwe
[d] Geological Survey of Namibia, Windhoek, Namibia

ARTICLE INFO

Article history:
Available online 29 March 2018

Keywords:
Botswana
Earthquake
Seismograph stations
Aftershocks
Intensity
Macroseismic

ABSTRACT

An earthquake of magnitude M_w 6.5 occurred on the evening of 3 April 2017 in Central Botswana, southern Africa. The event was well recorded by the regional seismic networks. The location by the Council for Geoscience (CGS) placed it near the Central Kgalagadi Game Reserve. Its effects were felt widely in southern Africa and were pronounced for residents of Gauteng and the North West Province in South Africa. In response to this event, the CGS, together with the Botswana Geoscience Institute (BGI), embarked on two scientific projects. The first project involved a macroseismic survey to study the extent and nature of the effects of the event in southern Africa. This involved CGS and BGI scientists soliciting information from members of the public through questionnaire surveys. More information was collected through questionnaires submitted online by the public. In total, 181 questionnaires were obtained through interviews and 151 online from South Africa, Zimbabwe and Namibia through collaboration between the CGS, the Meteorological Services Department of Zimbabwe and the Geological Survey of Namibia. All collected data were analysed to produce 79 intensity data points (IDPs) located all over the region, with maximum intensity values of VI (according to the Modified Mercalli Intensity scale) observed near the epicentre. This is quite a low value of maximum intensity for such a large event, but was expected given that the epicentral region is in a national park which is sparsely populated. The second scientific project involved the rapid installation of a temporary network of six seismograph stations in and around the location of the main event with the purpose of detecting and recording its aftershocks over a period of three months. Data recorded in the first month of April 2017 were collected and delivered to both the CGS and BGI for processing. More than 500 aftershock events of magnitude $M_L \geq 0.8$ were recorded and analysed for this period. All the events were located at the eastern edge of the Central Kgalagadi Park near the location of the main event in two clear clusters. The observed clusters imply that a segmented fault is the source of these earthquakes and is oriented in a NW-SE direction, similar to the direction inferred from the fault plane solution of the main event.

© 2018 Elsevier Ltd. All rights reserved.

1. Introduction

A major (M_W 6.5) earthquake occurred on 3 April 2017 at 19:40:13.4, South African Standard Time (SAST), in the Central Province of Botswana. The South African National Seismograph Network (SANSN) (Saunders et al., 2008) operated by the Council for Geoscience (CGS) recorded the event and located the epicentre near the south-eastern border of the Central Kgalagadi Game Reserve (Fig. 1). The earthquake was felt throughout southern Africa but with little damage reported mainly due to the remoteness of the epicentre from populated areas.

Botswana is characterized by a moderate level of seismic activity. Natural seismicity in the sub-continental region is fairly typical of stable continental regions (Kùlhánek and Meyer, 1979; Wright et al., 2003). The intraplate seismicity experienced in the country, like elsewhere in the rest of southern Africa, is characterized by a diffuse pattern of few moderate to large events (Fig. 1) per century, with a few concentrated clusters of modern-day seismicity

* Corresponding author.
E-mail address: vmidzi@geoscience.org.za (V. Midzi).

https://doi.org/10.1016/j.jafrearsci.2018.03.027
1464-343X/© 2018 Elsevier Ltd. All rights reserved.

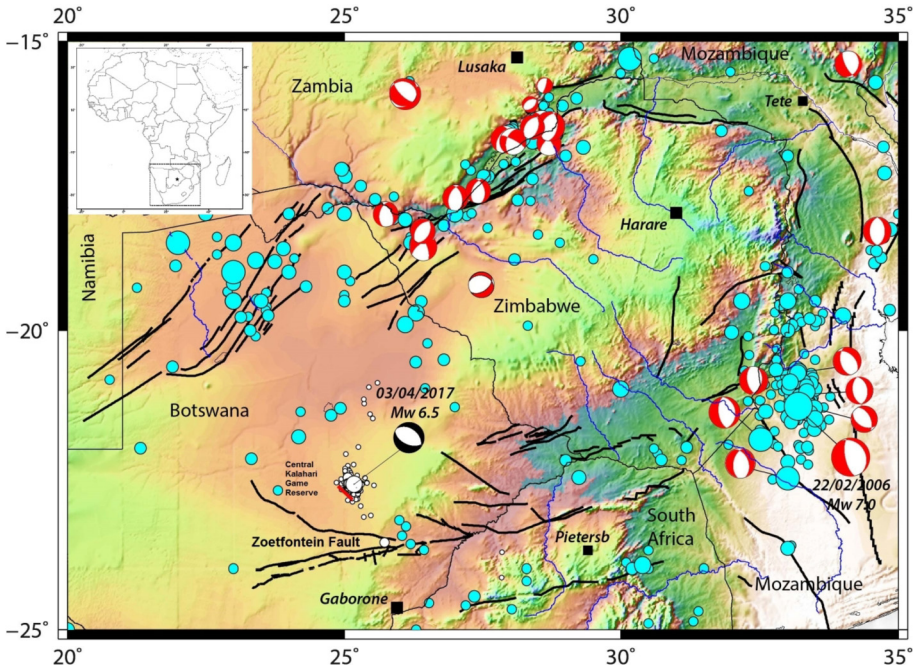

Fig. 1. The seismotectonics of central southern Africa showing the location of the Botswana 3 April 2017 earthquake (large white dot). Also shown is the fault plane solution of the event as well as fault plane solutions of other events in the region. Earthquakes shown in blue are of magnitude greater than or equal to 4.0 (Meghraoui et al., 2016), whilst the small white dots represent locations of aftershocks of the main Botswana earthquake. Inset shows a map of Africa with the region of study, southern Africa, indicated by the square box. Map modified from the Seismotectonic Map of Africa (Meghraoui et al., 2016).

(Graham et al., 1995, 1999; Wright et al., 2003). The locality of Botswana within the intraplate region of the southern part of the African Plate places the country thousands of kilometres away from the seismically active plate boundaries along mid-oceanic ridges in the South Atlantic and in the Southwest Indian oceans. On a global scale, this intraplate region experiences a relatively sparse, randomly scattered and unpredictable seismicity (Andreoli et al., 1996). Earthquakes of magnitude greater than 7.0 are rare in the country and across southern Africa. Most of the tectonic earthquakes in the interior of southern Africa are associated with the East African rift system (EARS), which is one of the most seismically active zones in the world. Previous studies of the seismicity of southern Africa indicated that the Okavango delta region (ODR) in the northwestern part of Botswana is one of the most seismically active areas in the subcontinent (e.g., Reeves, 1971, 1972).

Although Botswana is not well-known as an earthquake prone country due to the relatively low levels of local seismicity, the country has experienced unexpected moderate to large earthquakes especially in the ODR where an earthquake of magnitude 6.7 was observed on 11 October 1952 (Hutchins et al., 1976; Scholz et al., 1976; Reeves, 1971, 1972).

In response to the 3 April 2017 event, the CGS, in collaboration with colleagues from the Botswana Geoscience Institute (BGI), the Meteorological Services Department (MSD) of Zimbabwe and the Geological Survey of Namibia (GSN) embarked on two scientific surveys, *viz*: to collect macroseismic information to delineate the effect of ground shaking in the region, and to monitor the aftershocks following the main earthquake. Macroseismic data were collected through interviews and online questionnaires submitted to the CGS, MSD and GSN. At the same time, the CGS and BGI mobilised and installed a network of 6 temporary seismic stations to monitor the aftershock activity. The aim was to obtain data that was hoped would reduce the uncertainty associated with the aftershock hypocentre locations to help identify and delineate the causative structure of the seismicity.

2. Regional geological and tectonic framework

Much of Botswana and the rest of southern Africa are underlain by the Kalahari craton, which consists of the Archean Kaapvaal and Zimbabwe cratons that are cemented together by the 500 km ENE-WSW-trending Neoarchean Limpopo belt. The Limpopo Belt consists of highly metamorphosed granite-greenstone and granulite terrains which underwent a series of orogenic events between 2.0 and 3.0Ga (Adams and Nyblade, 2011). To the south, the Kaapvaal Craton is bordered by the Proterozoic Namaqua-Natal belt, which is a band of igneous and metamorphic rocks from the Namaqua or Kibaran Orogeny (1.0–1.2 Ga). The Namaqua-Natal belt is separated on its north-eastern boundary from the Kaapvaal Craton by the Kheis Province (Fig. 2), a fold-thrust belt of low-grade metamorphosed supracrustal rocks, with structures thought to pre-date the Namaqua Orogeny (approx. 2.0 Ga; Moen, 1999; Eglington and Armstrong, 2004). The complex region flanking the Zimbabwe Craton west and northwest of the Limpopo Belt is referred to as the Okwa-Magondi terrane (Fig. 2), although the regional geology remains enigmatic mainly because of the obscurity of geological features by extensive Kalahari sand cover (Carney et al., 1994). The approximately 2 Ga events of the Okwa and Magondi Belts were recorded in the western Limpopo Belt during the same time period and imposed a strong overprint on the western sector of the Zimbabwe Craton where it extends into Botswana. The Magondi Belt has also been described as the southwestern branch of the East African Rift System (EARS) (e.g. Modisi et al., 2000; Sebagenzi and Kaputo, 2002; Bufford et al., 2012) and is said to consist of a network of 100 km long and 40–80 km wide Quaternary rift basins distributed along an approximately 250 km wide corridor.

To the north and northeast, the super-craton is flanked by the Neoproterozoic Zambezi and Mozambique belts, both respectively western and southern extensions of the EARS. In the east, the Cratons are bordered by the Jurassic Lebombo monocline that is associated with the break-up of Gondwana (de Wit et al., 1992).

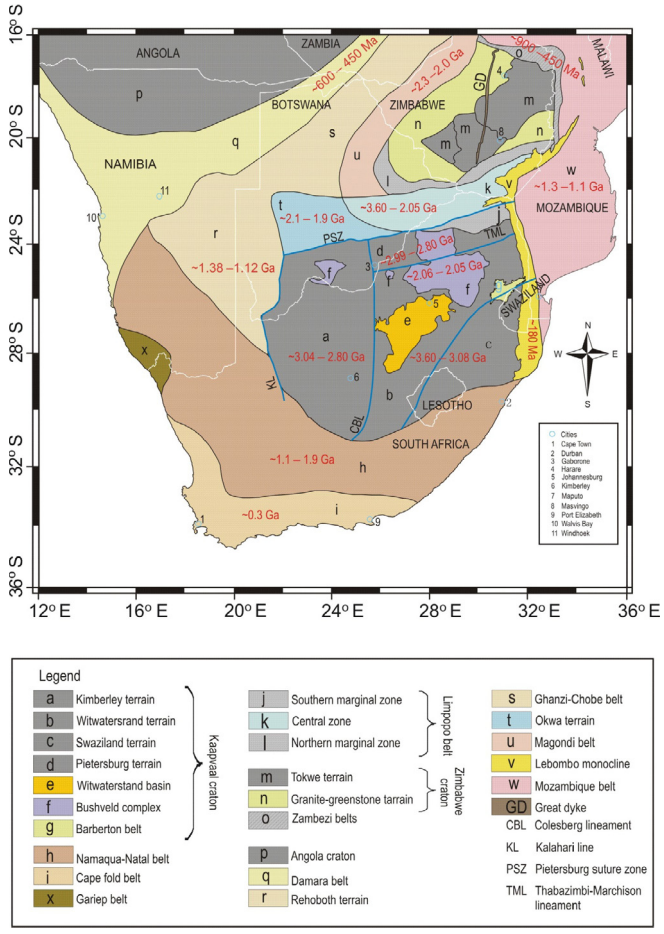

Fig. 2. Map showing generalized distribution of the major crustal blocks underlying southern Africa (from Kwadiba et al., Unpublished results).

Prior to the Mesozoic fragmentation of Gondwanaland, southern Africa constituted a part of the Gondwana supercontinent, which incorporated the remainder of the African continent as well as Antarctica, Australia, India, Madagascar and South America (Windley, 1981; Anhaeusser, 1990).

The occurrence of natural earthquakes in the region appears to be guided by the various blocks discussed above, with events mostly located in the mobile belts. Most events in Botswana have previously been associated with the ODR, which is located in the Ghanzi – Chobe and Magondi mobile belts. It has become clear from the 3 April 2017 event and its aftershocks that faults along the extension of the Limpopo belt into the south-eastern Botswana are also active and explain the scattered historical events in the area.

3. Data acquisition and analysis of the earthquake sequence

3.1. Fault plane solution

Fault plane solutions of the 3 April 2017 event were determined independently with the FOCMEC algorithm (Snoke, 2003) and the FPFIT code (Reasenberg and Oppenheimer, 1985) from 42 first motion P-phase arrivals using a 2° increment search. Details of stations used in the determination of the fault plane solutions are listed in Table 1. The Table indicates the distance from the epicentre as well as the Federation of Digital Seismograph Network (FDSN) codes (https://www.fdsn.org/). Station codes which are not FDSN registered are indicated by a superscript asterisk (Table 1). Fig. 3 shows the resulting fault plane solutions determined during this study. The solutions show that the event occurred on a normal fault oriented in a NW – SE direction. The nearest mapped fault located near this location is the NW-SE branch of the Zoetfontein fault as published in the Seismotectonic map of Africa (Meghraoui et al., 2016). There is a strong possibility that a similar fault to the east of this branch was the source of the event, given that the area appears to be active as shown by the scattering of moderately sized events (Fig. 1). It should be noted that no faults with a visible surface expression have been mapped in the area due to the thick surface sand cover in the area.

Table 1
Stations used in determining the fault plane solutions. *Not FDSN registered.

Station	Network Code	Distance (km)	Country
LEPH	ZA	308	South Africa
MUSN	ZA	488	South Africa
SWZ	ZA	512	South Africa
PRYS	ZA	534	South Africa
CRLN	ZA	625	South Africa
PILG	ZA	626	South Africa
MOPA	ZA	650	South Africa
SNKL	ZA	686	South Africa
NWCL	ZA	747	South Africa
UPI	ZA	752	South Africa
POGA	ZA	849	South Africa
HVD	ZA	892	South Africa
KSTD	ZA	985	South Africa
BFON	ZA	1034	South Africa
BRAK	ZA	1046	South Africa
GRAF	ZA	1079	South Africa
FRAZ	ZA	1102	South Africa
KOMG	ZA	1108	South Africa
CVNA	ZA	1123	South Africa
SOE	ZA	1126	South Africa
MERW	ZA	1176	South Africa
BUFB	ZA	1285	South Africa
CER	ZA	1327	South Africa
HRAO	A1	451	South Africa
MATJ	A1	1268	South Africa
NHAM	AF	343	South Africa
NYAT	AF	397	South Africa
HOED	AF	627	South Africa
BOSA	GT	671	South Africa
LBTB	GT	276	Botswana
DBIC	GT	4595	Cote d'Ivoire
HAGI	MG*	727	Swaziland
MALI	MG*	730	Swaziland
ARMS	NA*	814	Namibia
WIN	NA*	827	Namibia
KMBO	GE	2709	Kenya
SNAA	GE	5749	Antarctica
SUR	II	1169	South Africa
ABPO	II	2331	Madagascar
MBAR	II	2505	Uganda
SHEL	II	3321	St. Helena

3.2. Macroseismic survey

Macroseismic intensity data form an integral part of seismological, engineering and loss modelling and provide important information that can be used to reconstruct shaking distributions (Midzi et al., 2013). One of the main uses of this information is when selecting appropriate ground-motion prediction equations for seismic hazard assessments (Bakun and McGarr, 2002; Allen and Wald, 2009; Scherbaum et al., 2009; Delavaud et al., 2009).

A team of CGS scientists was dispatched on 4 April 2017 to conduct interviews in South African towns to collect macroseismic data that could be used to quantify the effects of the earthquake in South Africa. At the same time a team of BGI scientists also

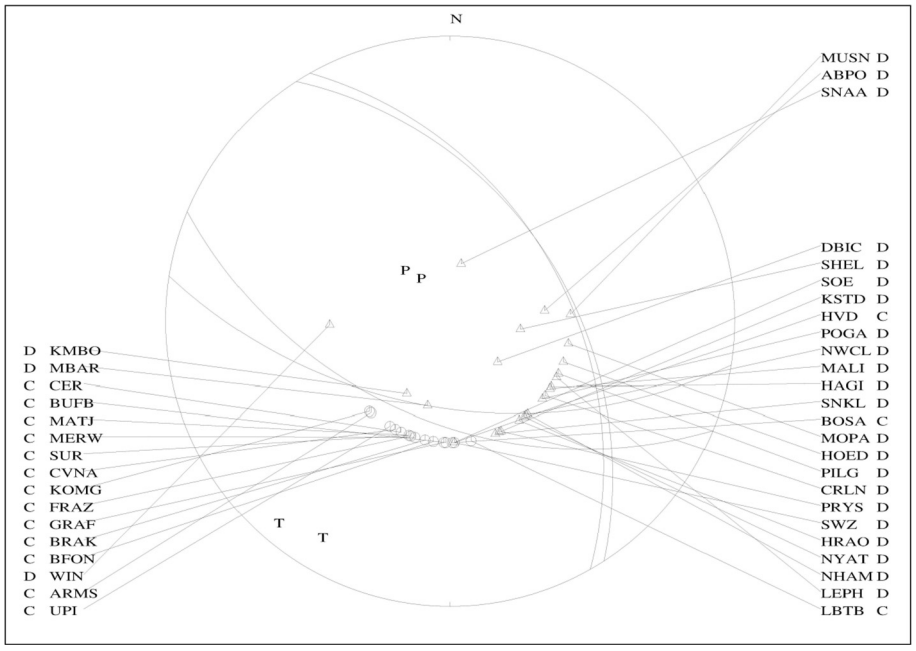

Fig. 3. Fault plane solutions determined with the FOCMEC code (Snoke, 2003) and FPFIT code (Reasenberg and Oppenheimer, 1985) from 42 first motion polarities. Codes of stations used and their polarities are shown in the figure. Triangles represent dilational polarities whilst circles represent compressional polarities. P and T are the Pressure and Tension axes respectively where the P axis reflects the maximum compressive stress direction and the T axis reflects the minimum compressive stress direction.

conducted a macroseismic survey in the epicentral area to identify possible damage caused by the event. No evidence of structural damage was seen since the event occurred in an isolated area devoid of human settlements. The only damage observed was at a mine located about 40 km west of the epicentral area where items such as ceilings, light fixtures (Fig. 4) and cupboards fell over. According to reports by some of the mine personnel, snakes were observed moving in a south western direction just before the main event occurred and then their tracks observed again later after the event but now moving back to the northeast. The mine staff also reported feeling strong shaking at the mine site which caused them to completely loose balance. However, no significant structural damage to their buildings occurred mainly because they are prefabricated structures which are flexible enough to move with the shaking. The lack of permanent settlements with brick houses in the region, which is in a desert and also in a national game park, clearly explains the lack of significant damage, injury or deaths of people.

Interviews were also conducted to gather macroseismic data from outlying towns in Botswana. In addition to questionnaires distributed through interviews, members of the public also submitted online questionnaires to the CGS, MSD and GSN resulting in a total of 322 questionnaires obtained. A total of 181 were obtained through interviews and the remainder (141) submitted online with their spatial distribution as shown in Fig. 5. The intensity information obtained through questionnaires is spatially distributed throughout southern Africa, with the majority from South Africa, Zimbabwe, Botswana and Namibia (Fig. 5).

The individual intensity indicators contained in the questionnaires for each place were summarised according to the methodology described by Midzi et al. (2013). Intensity values were assigned to sorted and grouped observations by comparing the summary of the observations for each place with the descriptions given for the intensity degrees on the Modified Mercalli Intensity scale, MMI-56 (Richter, 1958). In assigning intensity values, extreme care was taken to ensure that the correct assignment was the one that best expressed the generality of the observations (Musson and Cecić, 2002). Following the process described above, a total of 79 Individual Data Points (IDPs) were created (Fig. 6). As shown in Fig. 6, the highest intensity levels of VI were observed at places located close to the epicentre in central Botswana (14 km and 91 km from the epicentre). There is a notable difference in the intensity levels observed according to azimuth, with high values observed at places located in the northeast of the epicentre in Zimbabwe compared to those in the east and west at similar distance as in South Africa and Namibia (Fig. 6) respectively. Possible explanations for this phenomenon are the variations in the seismic wave attenuation of the crust in the areas in question and the modification of radiation pattern of the seismic wave energy by the source mechanisms. It must be noted that a fault acts like an antenna in radiating seismic energy.

A quality assessment of the IDPs, shows that 24 IDPs were each created using information from a single questionnaire only, thus, reducing the confidence in the results. However, most were created using information from multiple questionnaires, with five created using more than 10 observations each (Fig. 7). On average four observations were used to create each IDP.

3.3. Temporary network and aftershock distribution

The second aspect of the scientific response involved the monitoring of aftershocks linked to the M_W6.5 earthquake. In collaboration with scientists from BGI, the CGS identified six suitable sites where a network of seismographs was deployed (Fig. 8). Each station consisted of a Trillion Compact 20s broadband seismometer connected to a Centaur digitiser recording continuous waveforms at 250 s/s with GPS timing. The power supply relied on batteries charged using solar panels. Waveforms were stored on an external hard disk drive since mobile communication was not available for real time transmission of waveform data. The setup of the network, though suitable for the job, was not optimal as there were no stations east and southwest of the cluster. This was due to

Fig. 4. Typical damage to light fixtures observed at a mine located about 40 km from the Botswana 3 April 2017 earthquake epicentre.

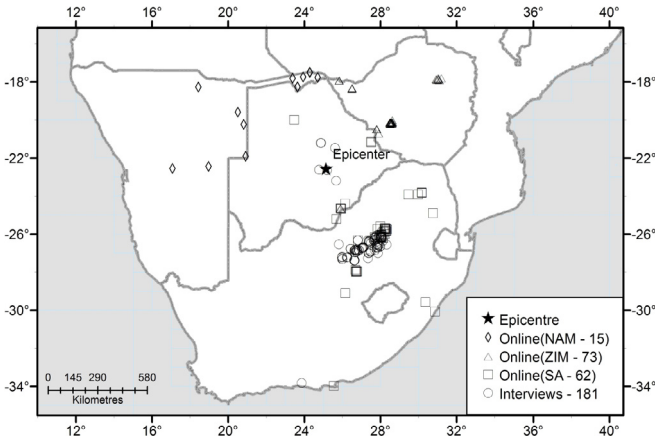

Fig. 5. Spatial distribution of questionnaires collected and analysed for the 3 April 2017 Botswana earthquake. The numbers shown in the legend represent the total number of each observation type obtained. The black star indicates the location of the main earthquake.

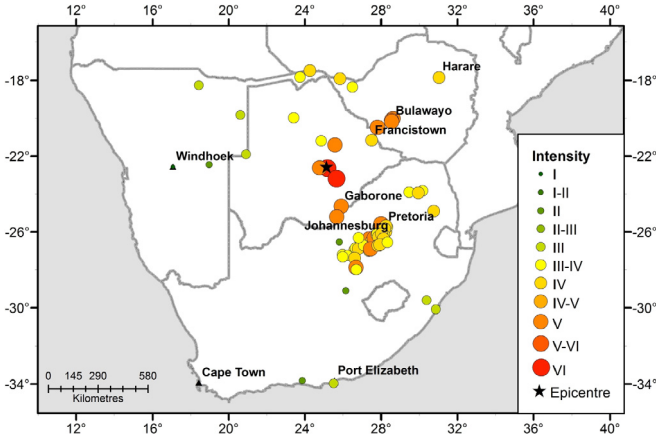

Fig. 6. The spatial distribution of IDPs obtained after analysis of collected macroseismic data of the 3 April 2017 Botswana earthquake. The black star indicates the location of the main earthquake. Observed is a notable difference in the intensity levels observed according to azimuth, with high values observed at places located in the northeast of the epicentre compared to those in the east and west.

the inaccessibility of the territory which was mainly in a sandy, but overgrown game reserve. This delayed the installation of the stations to beyond the time initially planned by the team.

The stations were deployed for a period of three months. A routine maintenance visit was undertaken during early May 2017, to download recorded data. The data, which included recordings from 8 to 30 April 2017, were analysed at the CGS. A total of 506 aftershocks were identified and analysed using the HYPOCENTER (Lienert and Havskov, 1995) code as implemented in the SEISAN Data Analysis Software (Ottemöller et al., 2015) resulting in epicentre locations with errors of about 2.5 km on average (Fig. 9). The analysed and plotted aftershocks (Fig. 10a) had local magnitude values (Saunders et al., 2013) ranging between M_L0.8 and M_L4.5. They were located in the same area as the main event of 3 April 2017 (Fig. 10).

The distribution of the aftershock activity exhibits a clear northwest-southeast orientation in two clusters of approximately 25 km and 19 km in length (Fig. 10). The two clusters suggest that the fault source of these events and possibly the main event constitute two fault segments.

A plot of the time distribution of the aftershocks, as shown in Fig. 10b, indicates a possible aftershocks sequence originating in the northern fault segment with most of the later events occurring in the southern larger cluster. The seismicity distribution shows a gradual decrease in seismic activity from 101 events on 8 August 2017 decreasing to ~20 events on 30 April 2017 (Fig. 11). The aftershock decay very likely reflects the stress readjustment following the stress change due to the mainshock (Ogata, 1998).

The north–south depth distribution of the aftershocks is shown in the cross section in Fig. 12 and also displays the aforementioned fault clusters. The shallower and smaller northern cluster shows events located at a depth less than 20 km, while hypocentral depths reach 30 km in the southern cluster. It should be noted that the depth values of aftershocks have errors of the order of 2.5 km on average (Fig. 12).

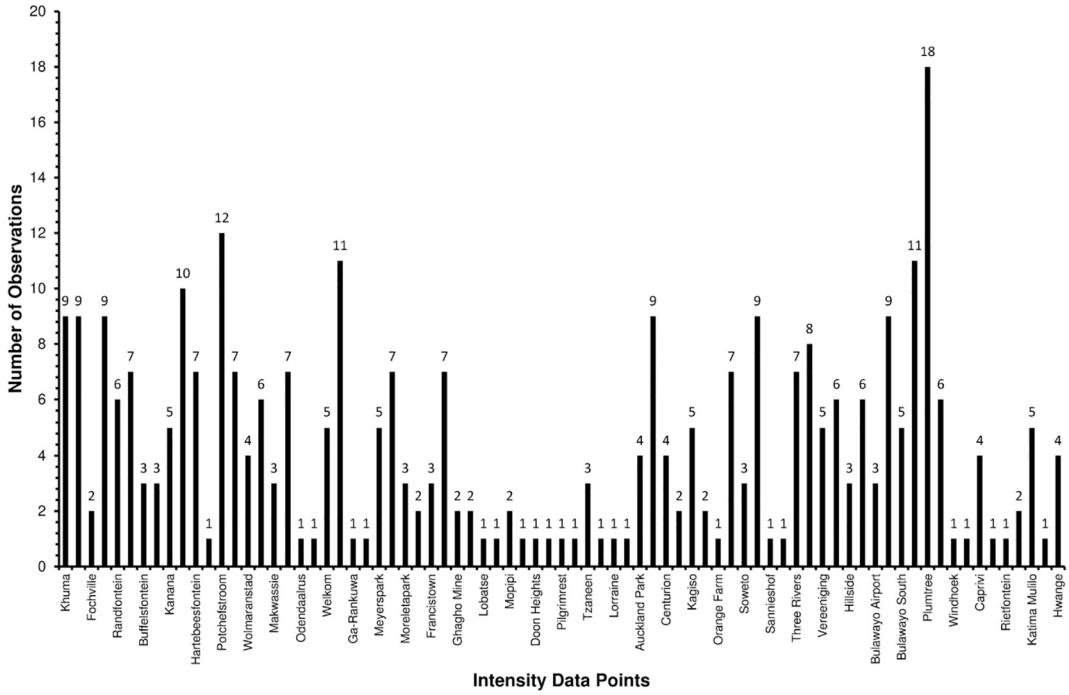

Fig. 7. Number of observations used to create each IDP.

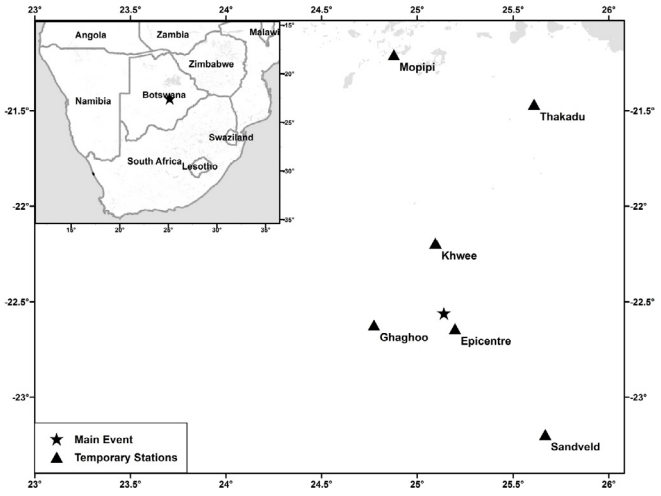

Fig. 8. Location of the six stations making up the temporary network in and around the Botswana 3 April 2017 earthquake epicentral area. Inset shows the regional map showing the location of the main event.

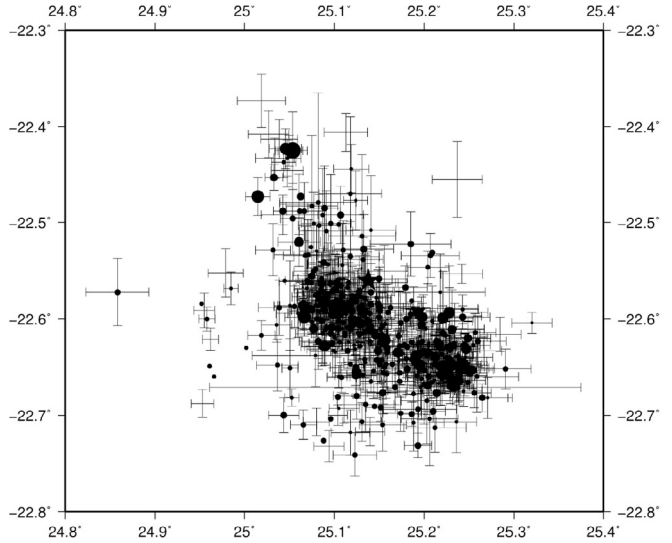

Fig. 9. Epicentre errors, which were observed to be about 2.5 km on average for both latitude and longitude.

4. Discussion and conclusion

The M_W6.5 Botswana earthquake is one of the largest instrumentally recorded events to occur within the Botswana territory. Though the event caused little to no damage, its effect was felt over a wide area (Figs. 5 and 6) and as far south as Port Elizabeth in South Africa.

The location of the aftershocks recorded soon after the occurrence of the earthquake enabled the delineation of the possible source rupture zone of the main event. A 50 km long northwest–southeast trending seismicity zone is revealed by the aftershock sequence and shows the possibility of two distinct segments of an active fault in central Botswana. Such a fault has not been mapped before but is probably linked to the regional faulting associated with the Zoetfontein faulting as in the seismotectonic map of Africa (Meghraoui et al., 2016) and shown in Fig. 1. At depth, a profile shows a large southern cluster between 20 and 30 km and a smaller northern cluster at about 20 km. The deeper southern cluster can be interpreted as acting on the same fault rupture as the main event.

The successful rapid scientific response and collaboration amongst organisations in southern Africa after the 3 April 2017 Botswana earthquake bodes well for future effective collaboration in the field of seismology in the region. It is hoped that this collaboration will open up avenues for further research linked to

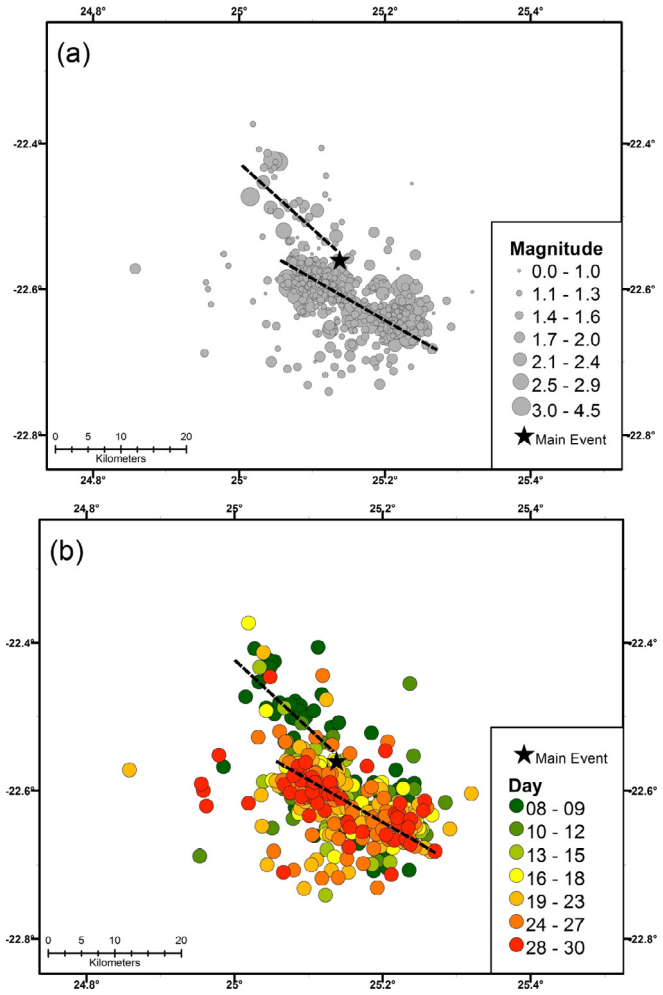

Fig. 10. Maps showing the spatial distribution of aftershocks of the 3 April 2017 Botswana earthquake plotted according to (a) magnitude and (b) time from 8 to 30 April 2017. Black broken lines represent general orientation of the clusters of aftershocks.

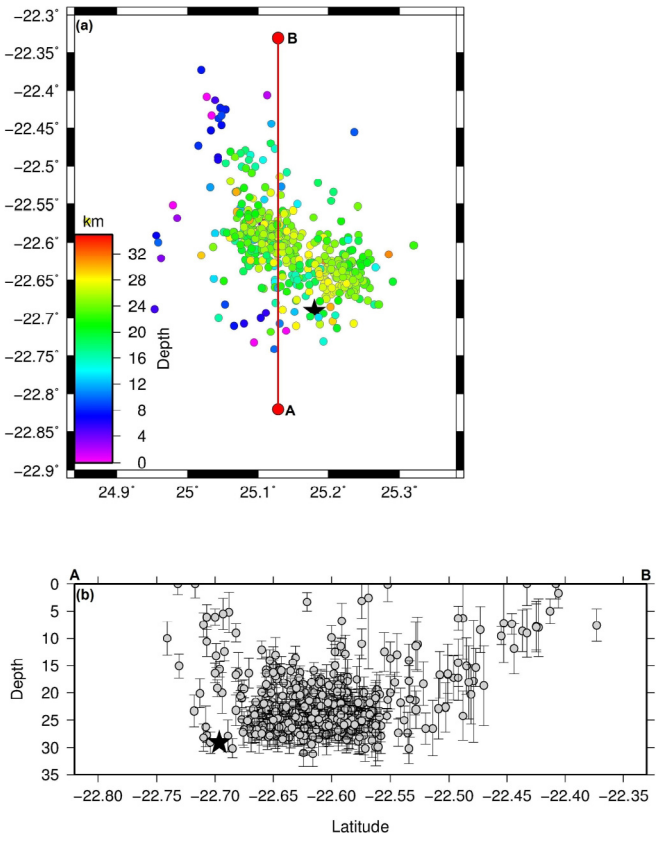

Fig. 12. Spatial distribution of aftershocks according to depth values with the black star representing the mainshock (a). In (b) is the aftershock profile showing their distribution at depth according to the line AB in (a). Also indicated are vertical bars representing errors in depth values of 2.5 km on average.

this and other events in the region to better understand the seismotectonics of southern Africa. The occurrence of moderate to large earthquake sequences in southern Africa is episodic (Manzunzu et al., 2017) and their record with dense seismic networks is quite recent (Fonseca et al., 2014). Thus the analysis of the 2017 Botswana

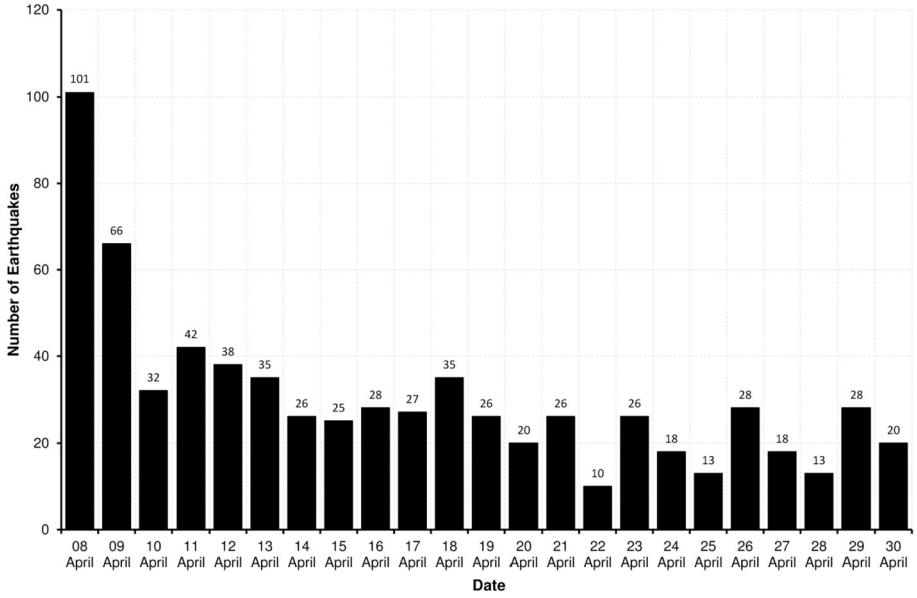

Fig. 11. Temporal variation in aftershock activity following the 3 April 2017 Botswana earthquake.

aftershock sequence will bring valuable insight into the occurrence of potentially damaging seismic events in the region.

Funding

The research did not receive any specific grant from funding agencies in the public, commercial, or not-for-profit sectors. However, the Council for Geoscience and the Botswana Geoscience Institute funded the work from internal research funds.

Acknowledgements

The authors are grateful for the quick positive response and financial assistance from the management of the Council for Geoscience and Botswana Geoscience Institute, which enabled us to rapidly respond to the earthquake and conduct the research reported here.

References

Musson, R.M.W., Cecić, I., 2002. Macroseismology. In: Lee, W.H.K., Kanamori, H., Jennings, P.C., Kisslinger, C. (Eds.), International Handbook of Earthquake and Engineering Seismology. International Geophysics, vol. 81, pp. 807–822. A.

Adams, A., Nyblade, A., 2011. Shear wave velocity structure of the southern African upper mantle with implications for the uplift of southern Africa. Geophys. J. Int. 186, 808–824.

Allen, T.I., Wald, D.J., 2009. Evaluation of ground-motion modelling techniques for use in Global ShakeMap: a critique of instrumental ground motion prediction equations, peak ground motion to macroseismic intensity conversions, and macroseismic intensity predictions in different tectonic settings. US Geological Survey Open-File Report 2009–1047, 114.

Andreoli, M.A.G., Doucouré, M., van Bever Donker, J., Brandt, D., Andersen, N.J.B., 1996. Neotectonics of southern Africa — a review. Afr. Geosci. Rev. 3, 1–16.

Anhaeusser, C.R., 1990. Precambrian crustal evolution and metallogeny of southern Africa. In: Naqvi, S.M. (Ed.), Precambrian Continental Crust and its Economic Resources. Elsevier, Amsterdam, pp. 123–156.

Bakun, W.H., McGarr, A., 2002. Differences in attenuation among the stable continental regions. Geophys. Res. Lett. 29 (23) https://doi.org/10.1029/2002GL015457.

Bufford, K.M., Atekwana, E.A., Abdelsalam, M.G., Shemang, E., Atekwana, E.A., Mickus e, K., Moidaki, M., Modisi, M.P., Molwalefhe, L., 2012. Geometry and faults tectonic activity of the Okavango Rift Zone, Botswana: evidence from magnetotelluric and electrical resistivity tomography imaging. J. Afr. Earth Sci. 65, 61–71.

Carney, J.N., Aldiss, D.T., Lock, N.P., 1994. The geology of Botswana. Bulletin of the Geological Survey of Botswana 37, 113.

de Wit, M.J., Roering, C., Hart, R.J., Armstrong, R.A., de Ronde, C.E.J., Green, R.W.E., Tredoux, M., Perberdy, E., Hart, R.A., 1992. Formation of an archean continent. Nature 357, 553–562.

Delavaud, E., Scherbaum, F., Kuehn, N., Riggelsen, C., 2009. Informationtheoretic selection of ground-motion prediction equations for seismic hazard analysis: an applicability study using Californian data. Bull. Seismol. Soc. Am. 99 (6), 3248–3263.

Eglington, B.M., Armstrong, R.A., 2004. The Kaapvaal Craton and adjacent orogens, southern Africa: a geochronological database and overview of the geological development of the craton. S. Afr. J. Geol. 107, 13–32.

Fonseca, J.F.B.D., Chamussa, J., Domingues, A., Helffrich, G., Antunes, E., van Aswegen, G., Pinto, L.V., Custódio, S., Manhiça, V.J., 2014. MOZART: a seismological investigation of the east African rift in Central Mozambique. Seismol Res. Lett. 85 (1), 108–116.

Graham, G., Brandt, M.B.C., Ford, M., Saunders, I., Brink, L., 1995. Catalogue of Earthquakes in Southern Africa and Surrounding Oceans for 1990. Council for Geoscience, Pretoria, South Africa, p. 21.

Graham, G., Turza, M., Fernandez, L.M., 1999. Energy release of large earth tremors in three gold mining districts of South Africa: an analysis of the energy release rate. Southern African Geophysical Review 3, 1–7.

Hutchins, D.G., Hutton, L.G., Hutton, S.M., Jones, C.R., Loenhert, E.P., 1976. A summary of the geology, seismicity, geomorphology and hydrogeology of the Okavango Delta. Bulletin 7. Botswana Geological Survey Department.

Kùlhánek, O., Meyer, K., 1979. A Proposal for a Seismograph Station Network in Ngamiland, Botswana. Technical Report. Seismological Institute, Uppsala, Sweden.

Kwadiba, M.T.O, Durrheim, R.J., James, D.E., Wagner, L.S., Zhao, D., Lei, J., (Unpublished Results). Geotomography of the Uppermost Crust-mantle System beneath the Kalahari Craton from Local and Regional P-waves.

Lienert, B.R.E., Havskov, J., 1995. A computer program for locating earthquakes both locally and globally. Seismol Res. Lett. 66 (5), 26–36.

Manzunzu, B., Midzi, V., Mangongolo, A., Essrich, F., 2017. The aftershock sequence of the 5 August 2014 Orkney earthquake (ML 5.5), South Africa. J. Seismol. https://doi.org/10.1007/s10950-017-9667-z.

Meghraoui, M., Amponsah, P., Ayadi, A., Ayele, A., Ateba, B., Bensuleman, A., Delvaux, D., El Gabry, M., Fernandes, R., Midzi, V., Roos, M., Timoulali, Y., 2016. The seismotectonic map of Africa. Episodes 10 (1), 9–18. https://doi.org/10.18814/epiiugs/2016/v39i1/89232.

Midzi, V., Bommer, J.J., Strasser, F.O., Albini, P., Zulu, B.S., Prasad, K., Flint, N.S., 2013. An intensity database for earthquakes in South Africa from 1912 to 2011. J. Seismol. 17, 1183–1205.

Modisi, M.P., Atekwana, E.A., Kampunzu, A.B., Ngwisanyi, T.H., 2000. Rift kinematics during the incipient stages of continental extension: evidence from the nascent Okavango rift basin, northwest Botswana. Geology 28, 939–942.

Moen, H.F.G., 1999. The Kheis Tectonic province, southern Africa: a lithostratigraphic perspective. S. Afr. J. Geol. 102, 27–42.

Ogata, Y., 1998. Space-time point-process model for earthquake occurrences. Ann. Inst. Stat. Math. 50 (2), 379–402.

Ottemöller, L., Voss, P., Havskov, J., 2015. The SEISAN Earthquake Analysis Software for the Windows, Solaris, Linux and MACOSX. University of Bergen, Bergen, Norway, p. 402.

Reasenberg, P., Oppenheimer, D., 1985. Fp_t, fpplot, and fppage: Fortran computer programs for calculating and displaying earthquake fault plane solutions. Technical report. U.S. Geological Survey.

Reeves, C.V., 1971. The Seismicity of Botswana. Department of Geological Survey Internal Report CVR/1/71, Lobatse, Botswana.

Reeves, C.V., 1972. Rifting in the Kalahari? Nature 237, 95–96.

Richter, C., 1958. Elementary Seismology. Freeman, San Franscisco, U.S.A, p. 578.

Saunders, I., Brandt, M.B.C., Steyn, J., Roblin, D., Kijko, A., 2008. the South african national seismograph network. Seismol Res. Lett. 79 (2), 203–210.

Saunders, I., Ottemöller, L., Brandt, M.B.C., Fourie, C.J.S., 2013. Calibration of an ML scale for South Africa using tectonic earthquake data recorded by the South African National Seismograph Network: 2006 to 2009. J. Seismol. 17, 437–451.

Scherbaum, F., Delavaud, E., Riggelsen, C., 2009. Model selection in seismic hazard analysis: an information-theoretic perspective. Bull. Seismol. Soc. Am. 99 (6), 3234–3247.

Scholz, C.H., Koczynski, T.A., Hutchins, D.G., 1976. Evidence for incipient rifting in southern Africa. Geophys. J. Roy. Astron. Soc. 44, 135–144.

Sebagenzi, M.N., Kaputo, K., 2002. Geophysical evidence of continental break up in the southeast of the democratic republic of Congo and Zambia (central Africa). In: Cloetingh, S.A.P.L., Ben-Avraham, Z. (Eds.), From Continental Extension to Collision: Africa–europe Interaction, the Dead Sea and Analogue Natural Laboratories. EGU (European Geosciences Union), Stephan Mueller Special Publication Series, vol. 2, pp. 193–206.

Snoke, J.A., 2003. FOCMEC: focal mechanism determinations. In: Lee, W.H.K., Kanamori, H., Jennings, P.C., Kisslinger, C. (Eds.), International Handbook of Earthquake and Engineering Seismology. Academic Press, San Diego, California, p. 994.

Windley, B.F., 1981. Precambrian rocks in the light of the plate-tectonic concept. In: Kröner, A. (Ed.), Tectonics. Elsevier, Oxford, pp. 1–20.

Wright, C., Kgaswane, E.M., Kwadiba, M.T.O., Simon, R.E., Nguuri, T.K., McRae-Samuel, R., 2003. South African seismicity, April 1997 to April 1999, and regional variations in the crust and uppermost mantle of the Kaapvaal craton. In: Jones, A.G., Carlson, R.W., Grutter, H. (Eds.), A Tale of Two Cratons: the Slave-kaapvaal Workshop. Lithos, vol. 71, pp. 369–392.